

DROP COALESCENCE AND BREAK-UP THROUGH THE RHOD-SPH

M. Antuono, S. Marrone, A. Colagrossi
 Institute of Marine Engineering
 National Research Council of Italy, CNR-INM
 Rome, Italy

I. INTRODUCTION

The present paper is dedicated to the study of coalescence and break-up phenomena of viscous drops with surface tension. The fluid is assumed to be Newtonian and, therefore, is described through the Navier-Stokes equations (NSEs). The work is carried on through the use of the RHOD-SPH scheme defined in [1] (we address the reader to this paper for details on the numerical model) and relies on the analysis of the energy balance during the above-mentioned phenomena.

Hereinafter, we disregard the presence of solid boundaries and assume that the boundary is a free surface, namely $\Omega = \Omega_F$. Hence, the energy equation of the NSEs is:

$$\frac{D}{Dt} \int_{\Omega} \rho_0 \frac{\|\mathbf{u}\|^2}{2} dV = \sigma \int_{\partial\Omega_F} \kappa (\mathbf{u} \cdot \mathbf{n}) dS - 2\mu \int_{\Omega} \mathbb{D} : \mathbb{D} dV \quad (1)$$

where σ is the surface tension and κ is the curvature of the free surface. It is possible to show that the integral related to the surface tensions is equivalent to the material derivative of the surface area, namely:

$$\int_{\partial\Omega_F} \kappa (\mathbf{u} \cdot \mathbf{n}) dS = -\frac{D}{Dt} \left(\int_{\partial\Omega_F} dS \right) \quad (2)$$

This allows one to rearrange the energy equation in the following compact form:

$$\frac{D\mathcal{E}_K}{Dt} + \frac{D\mathcal{E}_\sigma}{Dt} = \mathcal{P}_v \quad (3)$$

where \mathcal{E}_K is the kinetic energy, $\mathcal{E}_\sigma = \sigma \mathcal{L}_F$ is the surface tension energy (here \mathcal{L}_F is the free-surface area) and, finally, \mathcal{P}_v indicates dissipated by viscous effects. Since we do not consider external forcing terms, the flows studied in the present work only depends on the Reynolds and Weber numbers defined as:

$$\text{Re} = \frac{\rho_0 U_{ref} L}{\mu}, \quad \text{We} = \frac{\rho_0 U_{ref}^2 L}{\sigma}$$

where U_{ref} and L are the reference velocity and length of the problem at hand respectively.

A. The surface-tension model

The Continuum Surface Force (CSF) model described in [2] has been implemented in the RHOD-SPH scheme. In particular, the surface tension force \mathbf{F}_i^σ is given below:

$$\begin{cases} \mathbf{F}_i^\sigma &= \sigma \kappa_i \mathbf{n}_i \delta_{Fi}, & \delta_{Fi} = 2 \left\| \sum_j \nabla_i W_{ij} V_j \right\| \\ \kappa_i &= \mathbb{L}_i \sum_j (\mathbf{n}_i - \mathbf{n}_j) \cdot \nabla_i W_{ij} V_j, & \mathbf{n}_i = -\frac{\nabla \lambda_i}{\|\nabla \lambda_i\|}, \\ \nabla \lambda_i &= \mathbb{L}_i \sum_j (\lambda_j - \lambda_i) \nabla_i W_{ij} V_j, \end{cases} \quad (4)$$

where λ_i is the minimum eigenvalue of \mathbb{L}_i^{-1} and \mathbb{L}_i is the renormalization matrix. As in [2], four critical corrections necessary for the description of thin jets or small drops are also implemented in order to increase accuracy and robustness of the scheme. The above scheme has been further validated in [3], proving to be robust and accurate.

B. Energy balance of the RHOD-SPH model

The energy balance of the RHOD-SPH model is rather complex because of the presence of power terms related to the use of the shifting velocity and Riemann fluxes. In the present work, however, we mainly focus on the action played by the surface tension force. Hence, for this reason and for the ease of the treatise, some of the remaining terms of the energy equation are introduced without giving their whole expressions. In any case, more details can be found in [1].

The energy balance of the particle system can be rewritten as:

$$\begin{cases} \frac{D\mathcal{E}_K}{Dt} + \frac{D\mathcal{E}_C}{Dt} = \mathcal{P}_{diss} + \mathcal{P}_\sigma, & \mathcal{E}_K = \sum_i m_i \frac{\|\mathbf{u}_i\|^2}{2}, \\ \mathcal{E}_C = \sum_i m_i \int_{\rho_0}^{\rho_i} \frac{p(s)}{s^2} ds, & \mathcal{P}_\sigma = \sum_i (\mathbf{F}_i^\sigma \cdot \mathbf{u}_i), \\ \mathcal{P}_v = \sum_i (\mathbf{F}_i^\mu \cdot \mathbf{u}_i), & \mathcal{P}_{diss} = \mathcal{P}_v + \mathcal{P}_N, \end{cases} \quad (5)$$

where \mathcal{E}_C is the (reversible) energy associated with the fluid compressibility, \mathcal{P}_σ is the power of the surface tension force, \mathcal{P}_v is the power dissipated by the viscous effects and, finally, \mathcal{P}_N is

the power due to the action of the remaining numerical terms (mainly the particle shifting terms and the Riemann fluxes). In principle, this latter term has not a definite sign, but it always works as a dissipation in the numerical scheme. For this reason, we denote by $\mathcal{P}_{diss} = \mathcal{P}_v + \mathcal{P}_N$ the overall power dissipated by the numerical scheme.

Before proceeding, we introduce the energy dissipated by the RHOD-SPH and the work done by the surface tension force as:

$$Q_{diss} = \int_{t_0}^t \mathcal{P}_{diss} d\tau, \quad \mathcal{W}_\sigma = \int_{t_0}^t \mathcal{P}_\sigma d\tau. \quad (6)$$

According to the equation (2), \mathcal{P}_σ should be equal to $(-D\mathcal{E}_\sigma/Dt)$ and, consequently, \mathcal{W}_σ should be equal to $(\mathcal{E}_{\sigma 0} - \mathcal{E}_\sigma)$. Nonetheless, this is not true numerically, since the reversibility of \mathcal{W}_σ cannot be guaranteed in the adopted SPH model. In fact, the work \mathcal{W}_σ is intrinsically related to the CSF model which is based on the evaluation of local quantities (like the normal and the curvature of the free-surface), without any direct connection with global quantities, like the surface energy associated to the deformation of $\partial\Omega_F$.

In order to check the numerical error of the SPH scheme in the evaluation of the surface energy, \mathcal{E}_σ is evaluated through a Level-Set function ϕ . The latter is obtained by using the algorithm described in [4] based on the interpolation of the particles set on a Cartesian mesh. When the contour level $\phi = 0$ is extracted, it is possible to evaluate the perimeter of the drop \mathcal{L}_F and, therefore, the surface energy $\mathcal{E}_\sigma = \sigma\mathcal{L}_F$. It is worth noting that the Level-Set function is evaluated during a post-processing stage and for a limited number of time instants. Because of the CPU costs, it is not calculated at runtime for each time iteration.

Thanks to the above approach, at the end of each simulations it is possible to check to what extent the work \mathcal{W}_σ deviates from $(\mathcal{E}_{\sigma 0} - \mathcal{E}_\sigma)$ and if the deviation from the theoretical equality ultimately decreases when the spatial resolution $N = L/\Delta x$ increases. Note that the surface energy \mathcal{E}_σ is always evaluated geometrically through the Level-Set function ϕ , whereas the work of the surface tension forces \mathcal{W}_σ is evaluated from the CSF model that is embedded in the SPH scheme.

About the energy associated with the fluid compressibility, namely \mathcal{E}_C , this maintains small during the evolution as a consequence of the weak-compressibility assumption.

II. COALESCING DROPS

Two circular drops of radius R approaching each other with a constant velocity U_0 are set at an initial distance equal to the kernel radius R_W . The initial surface tension energy of the fluid system is $\mathcal{E}_{\sigma 0} = 2\pi\sigma R$, while its asymptotic value for long times is assumed to be that associated with a single circular drop generated by the merging of the initial drops. Since the latter drop has radius $R_\infty = \sqrt{2}R$, the asymptotic energy of the surface tension is $\mathcal{E}_{\sigma\infty} = \sqrt{2}\pi\sigma R$. and, therefore, the overall variation of surface tension energy is $\Delta\mathcal{E} = (\mathcal{E}_{\sigma 0} - \mathcal{E}_{\sigma\infty}) = 2\pi\sigma R(2 - \sqrt{2})$.

Denoting by M_0 the initial mass of the fluid system, we define the reference velocity of the problem as:

$$U_{ref} = \sqrt{\frac{\Delta\mathcal{E}}{M_0}} = \sqrt{\frac{\sigma(2 - \sqrt{2})}{R}} \quad (7)$$

By definition, this implies $We = (2 - \sqrt{2})$, while the Reynolds number has been set equal to 242. These values correspond, for example, to a water drop of 1 mm radius.

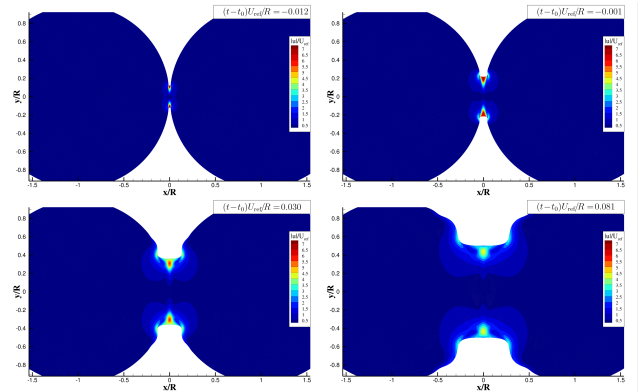


Fig. 1. Coalescing drops: early stages of the evolution for $We = (2 - \sqrt{2})$, $Re = 242$ and spatial resolution $N = 800$. Link Video N°1.

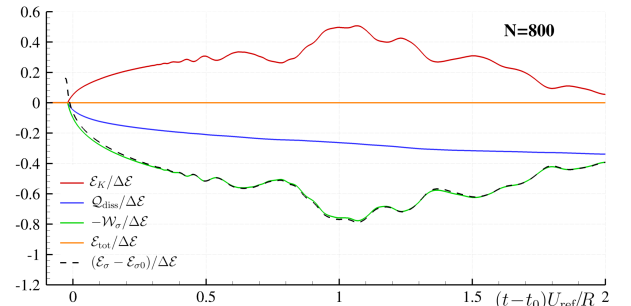


Fig. 2. Energy balance for the coalescing drops. The time history of the term $(\mathcal{E}_\sigma - \mathcal{E}_{\sigma 0})/\Delta\mathcal{E}$ has been shifted upward to match with the term $(-\mathcal{W}_\sigma/\Delta\mathcal{E})$ and show the initial gap caused by the coalescing phenomenon.

Hereinafter, $t_0 = 0.5R_W/U_{ref}$ indicates the theoretical time instant when the drops first touch. During the early stages of the evolution, large velocity values are observed at the extremities of the contact line (top panels of figure (1)). These values slowly decrease while the drops deform but remains localized close to the free surface.

Figure 2 displays the energy balance for the coalescing system. In this figure the time history of the surface tension energy, namely $(\mathcal{E}_\sigma - \mathcal{E}_{\sigma 0})/\Delta\mathcal{E}$, has been moved upward to match with the term $(-\mathcal{W}_\sigma/\Delta\mathcal{E})$. This allows us to highlight the generation of an energy gap at the initial time, i.e. when the drops first touch. In particular, during the early stages of coalescence, part of the free surface is trapped inside the two drop volumes, and two cusps are generated and propagate far from the initial contact point. This dynamics holds up until the

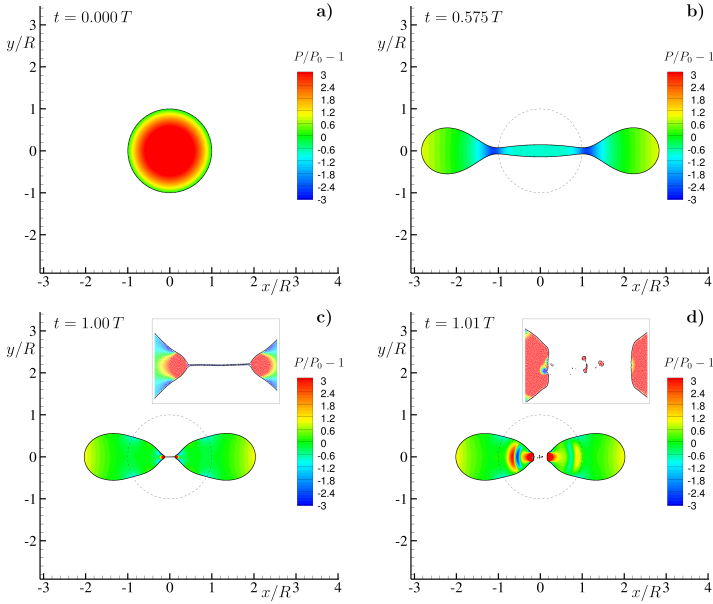


Fig. 3. Pressure evolution for a large amplitude oscillation of a 2D liquid drop. The spatial resolution is $N = R/\Delta r = 400$. Link Video N°2.

cusps disappear and a smooth surface develops. The length ℓ of the free surface that is incorporated inside the merged volumes leads to the energy gap $\delta\mathcal{E}_\sigma = \sigma\ell$ that is observed at the initial time in the Figure 2. This figure also shows that the total energy of the system, namely \mathcal{E}_{tot} , is conserved during the evolution. Such an energy term is obtained by integrating in time the first expression of the equation (5) and corresponds, in fact, to the summation of all the energy contributions, that is:

$$\mathcal{E}_{tot} = \mathcal{E}_K + \mathcal{E}_C - Q_{diss} - \mathcal{W}_\sigma. \quad (8)$$

Accordingly, \mathcal{E}_{tot} is monitored to check that the errors caused by the numerical time integration are negligible in comparison to the physical energy contributions.

III. BREAK-UP

We consider the case of a drop subjected to a two-mode oscillation of large amplitude, according to the analytical solution described in [5]. In particular we set $a = 1.25R$, $Re = 194$ and $We = 9.38$, which approximately corresponds to a water drop of radius $5.6 \cdot 10^{-5}m$. Figure 3 shows the main stages of the evolution of the oscillation drop for $N = R/\Delta r = 400$. The top right panel displays the maximum elongation of the initial drop in two bumps tied by a thin fluid thread. After this instant, the bumps start moving closer (bottom left panel), while the tread becomes thinner and thinner and eventually breaks (bottom right panel), generating tiny secondary drops and large acoustic waves that propagate inside the fluid bulk. Just before the breaking time the fluid tread is just two-particle thick, that is $2\Delta r = R/200$. After this stage, the two separated drops continue moving closer and, finally, merge.

A more detailed insight is provided by the analysis of the energy balance of the fluid system. This is illustrated in Figure

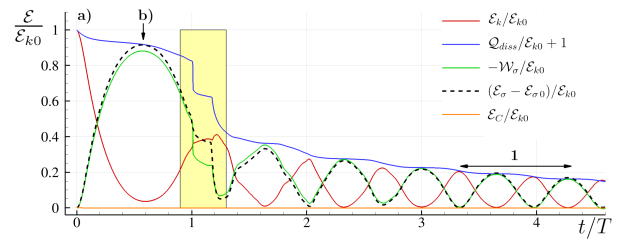


Fig. 4. Large amplitude oscillation of a 2D liquid drop: Top: long-time evolution of the main energy components for $N = 400$. The letters refer to the panels in Figure 3.

4 where the different energy components are shown. During the early evolution \mathcal{W}_σ and \mathcal{E}_σ show a good agreement. The overall behavior changes, however, when the break-up phenomenon occurs. In this case the work done by the surface tension forces, namely \mathcal{W}_σ , undergoes an abrupt discontinuity (Figure 4). This energy loss corresponds to the energy spent to separate the thin thread between the bumps. Conversely, the signal of the surface tension energy, \mathcal{E}_σ , maintains regular, since the overall length of the fluid system undergoes minor changes.

The opposite behavior is observed during the coalescence stage, that is when the drops reconnect after the break-up in the bottom-right panel of Figure 3. Indeed, the surface tension energy \mathcal{E}_σ experiences a sudden energy loss caused by the free-surface entrapment, in analogy to the dynamics described in Section §II. Conversely, the work \mathcal{W}_σ is less affected by the coalescence phenomenon, even though a larger dissipation is observed after the coalescence stage is completed. Remarkably, we observe that in the subsequent evolution \mathcal{W}_σ and \mathcal{E}_σ match together again, proving that the energy lost by \mathcal{W}_σ during the break-up is approximately equal to the energy lost by \mathcal{E}_σ during the coalescence stage.

ACKNOWLEDGMENT

This research was partially funded by the HASTA project (Grant No. 101138003) as part of the European Union Horizon research programme.

REFERENCES

- [1] J. Michel, A. Colagrossi, M. Antuono, and S. Marrone, “A regularized high-order diffusive smoothed particle hydrodynamics scheme without tensile instability,” *Physics of Fluids*, vol. 35, no. 10, 2023.
- [2] A. Vergnaud, G. Oger, D. Le Touzé, M. DeLefre, and L. Chiron, “C-CSF: Accurate, robust and efficient surface tension and contact angle models for single-phase flows using SPH,” *Computer Methods in Applied Mechanics and Engineering*, vol. 389, p. 114292, 2022.
- [3] S. Marrone, M. Antuono, A. Agresta, and A. Colagrossi, “A study on the energy consistency in sph surface tension modelling,” *Computer Methods in Applied Mechanics and Engineering*, vol. 433, p. 117473, 2025.
- [4] S. Marrone, A. Colagrossi, D. L. Touzé, and G. Graziani, “Fast free-surface detection and level-set function definition in SPH solvers,” *Journal of Computational Physics*, vol. 229, no. 10, pp. 3652–3663, 2010. [Online]. Available: <http://www.sciencedirect.com/science/article/pii/S0021999110000343>
- [5] A. Aalilija, C.-A. Gandin, and E. Hachem, “On the analytical and numerical simulation of an oscillating drop in zero-gravity,” *Computers & Fluids*, vol. 197, p. 104362, 2020.